THE JOURNAL OF PHYSICAL CHEMISTRY A

Article

pubs.acs.org/JPCA

Differential Cross Sections for the H + D_2 → HD(v' = 3, j' = 4−10) + D Reaction above the Conical Intersection

Hong Gao,[†] Mahima Sneha,[†] Foudhil Bouakline,[‡] Stuart C. Althorpe,[§] and Richard N. Zare*,[†]

[†]Department of Chemistry, Stanford University, Stanford, California 94305-5080, United States

[‡]Max-Born-Institute, Max-Born Strasse 2A, D-12489 Berlin, Germany

[§]Department of Chemistry, University of Cambridge, Lensfield Road, Cambridge CB2 1EW, United Kingdom

ABSTRACT: We report rovibrationally selected differential cross sections (DCSs) of the benchmark reaction H + D_2 → HD(v' = 3, j' = 4−10) + D at a collision energy of 3.26 eV, which exceeds the conical intersection of the H_3 potential energy surface at 2.74 eV. We use the PHOTOLOC technique in which a fluorine excimer laser at 157.64 nm photodissociates hydrogen bromide (HBr) molecules to generate fast H atoms and the HD product is detected in a state-specific manner by resonance-enhanced multiphoton ionization. Fully converged quantum wave packet calculations were performed for this reaction at this high collision energy without inclusion of the geometric phase (GP) effect, which takes into account coupling to the first excited state of the H_3 potential energy surface. Multimodal structures can be observed in most of the DCSs up to j' = 10, which is predicted by theory and also well-reproduced by experiment. The theoretically calculated DCSs are in good overall agreement with the experimental measurements, which indicates that the GP effect is not large enough that its existence can be verified experimentally at this collision energy.

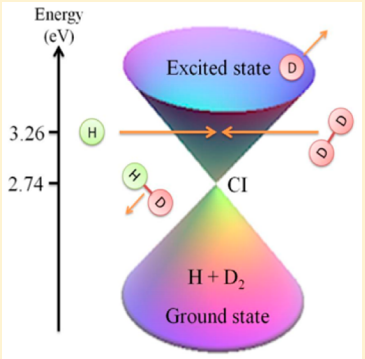

I. INTRODUCTION

The hydrogen-atom hydrogen-molecule exchange reaction H + H_2 → H_2 + H and its isotopic variants have served for many years as a benchmark reaction system for studying bimolecular reaction dynamics. Because it is the simplest neutral scattering system which contains only three electrons and three protons, a very accurate full dimensional potential energy surface (PES) can be obtained.[1] Fully converged time-dependent and time-independent quantum scattering calculations on this system are available, and nearly quantitative agreement with the experimental measurements has been achieved on the level of state-to-state differential cross sections (DCSs),[2−8] which has been believed to be one of the most sensitive tests of the validity of the PES and the corresponding scattering dynamics. Benefiting from the close collaboration between theory and experiment, a detailed and insightful picture of the scattering dynamics (both reactive and inelastic) about this prototype system has emerged, even though some discrepancies still exist.[9,10]

The unbound ground-state H_3 PES is connected to a bound excited-state PES via a conical intersection (CI) in the D_{3h} configuration (equilateral triangle geometry) with a minimum in the intersection seam at 2.74 eV. In the past, the scattering dynamics on this Jahn−Teller system has been confined to collision energies below the CI on the experimental side owing to technical difficulties. However, several theoretical studies have been made above the CI for the purpose of understanding nonadiabatic effects on the scattering dynamics arising from the participation of the first excited electronic potential surface.[11−14] One of the interesting nonadiabatic quantum effects arising from the presence of CI is the geometric phase (GP) effect. The GP effect arises from the fact that the electronic wave function will change sign whenever the nuclei complete an odd number of loops around the CI, which leads to a corresponding sign change in the nuclear wave function as the total wave function is required to be single-valued. How GP affects the collision dynamics of H + H_2 has been a long-standing problem ever since this interesting phenomenon was first discussed by Herzberg and Longuet-Higgins[15] in 1963 and Mead and Truhlar[16] in 1979. Many experimental and theoretical efforts have been devoted to this topic since then, and there have been contradictory assertions, which have generated much back-and-forth discussion. A detailed account of this can be found in a 2003 paper by Kendrick.[17] Recently, theory and experiment have started to converge to the same conclusion that the effect of GP on the state-to-state DCSs is negligible at low collision energies (<1.8 eV). Theory predicts that it is only at energies above 1.8 eV where the GP effect starts to show up in the state-to-state DCSs.[14,18,19] To the best of our knowledge, there have been no experiments to verify this claim so far. In this study, we investigate this benchmark collision system above the CI by using a fluorine excimer laser (157.64 nm) to photodissociate HBr in a supersonically

Special Issue: Dynamics of Molecular Collisions XXV: Fifty Years of Chemical Reaction Dynamics

Received: May 12, 2015
Revised: June 16, 2015
Published: June 19, 2015

DOI: 10.1021/acs.jpca.5b04573
J. Phys. Chem. A 2015, 119, 12036−12042

expanded mixture of HBr and D_2. This provides a collision energy of 3.26 eV for the H + D_2 reaction. We are motivated to make this study to explore possible nonadiabatic effects arising from the coupling between the two PESs, especially the GP effect. Rovibrationally selected DCSs are measured using the PHOTOLOC (photoinitiated reaction analyzed by the law of cosines) technique and are compared with fully converged quantum wave packet calculations. Presently, the agreement between experiment and theory that does not include GP is so sufficiently close that we cannot report the observation of a GP effect.

II. EXPERIMENTAL SECTION

The principle of the PHOTOLOC technique[20] and the construction of the three-dimensional (3D) ion imaging setup[21] have been described in detail before, and the experimental procedures are very similar to what have been used in several of our previous experiments;[7,8,10] consequently, only the details that are specific to the present experiment will be described here.

A mixture of HBr (~5%) in D_2 (Cambridge Isotope Laboratories, Inc. 99.6% D_2 + 0.4% HD) is supersonically expanded into the extraction region of a space-focused Wiley−McLaren time-of-flight mass spectrometer through a pulsed general valve (General Valve Series 9) which operates at the repetition rate of 10 Hz. The stagnation pressure in the valve is maintained at about 22 psi, and the supersonic expansion internally cools the D_2 molecules to (v = 0, j = 0−2) states. First, the molecular beam is perpendicularly intersected by the focused (through a CaF_2 spherical plano-convex lens with f = 42 cm) vacuum ultraviolet (VUV) laser beam from the fluorine excimer laser (Coherent, ExciStar-XS), which photodissociates the HBr molecules and initiates the reaction to form HD(v', j') products. After a delay of 15−20 ns, a counterpropagating focused (f = 50 cm) UV beam is used to state-selectively ionize the HD product via resonance-enhanced multiphoton ionization (REMPI) on the Q branch of the (3, 0) band of the $E,F\ ^1\Sigma_g^+ - X\ ^1\Sigma_g^+$ transition. The UV beam has a typical power of 650 μJ per pulse and is generated by doubling (with a BBO crystal) the output of a dye laser (Lambda Physik, LPD3000) pumped by the third harmonic output of a Nd:YAG laser (Quanta-Ray, DCR-3). The wavelength of the UV beam is scanned back and forth to cover the whole Doppler profile of the HD products. The lab frame speed of the HD ions is measured by using the three-dimensional ion imaging setup described in previous experiments and converted to a DCS based on the PHOTOLOC technique.

There are three aspects that make this experiment much harder than previous experiments. (1) The VUV beam (photolysis) cannot propagate in air; hence, the light path outside the chamber needs to be continuously purged by high-purity nitrogen gas. This condition limits the freedom of tuning and manipulating the VUV beam. Consequently, we usually fix the position of the VUV beam and tune the UV beam (probe) to make them spatially overlap in the interaction region. It is not a trivial task to obtain good overlap of the two laser beams spatially in the interaction region. Considering the relatively large photon energy difference between the VUV and UV lasers, it is impossible to use the method based on the two-color REMPI of the H_2, HD, or D_2 molecules, like we did previously[7] to overlap the two laser beams in the interaction region. We attached a small piece of white paper to a linear motion feedthrough to insert the paper into the interaction region and look at the beam positions as they fluoresce on the paper. Once we are convinced that the photolysis and probe beams overlap well, we remove the paper from the interaction region through the linear motion feedthrough. (2) The beam shape of the VUV laser generated by the excimer laser is in a rectangular shape and has different convergences in the horizontal and vertical directions. The spherical lens can focus it to only a line-shaped beam (~4 mm in length) in the interaction region; on the other side, the UV beam can be focused to a very small point. This makes the overlap between the two beams very inefficient; thus, the real signal is very weak in this experiment. (3) In spite of the low effective power, the VUV beam generates huge stray light noise on the MCP detector because its sensitivity is higher at this wavelength. To reduce this stray light noise to an acceptable level, we used optical baffles on both sides of the chamber to confine the VUV beam, and we also used Brewster windows to prevent the VUV beam from reflecting back into the interaction region. In addition, the VUV beam strongly ionizes D_2, HD, HBr, and Br in the beam which can lead to space charge effects. Consequently, we must limit the power of the photolysis beam to be ~300 μJ per pulse in the interaction region, which makes it impossible to increase the signal level by using a higher photolysis laser power.

The VUV beam can ionize the 0.4% HD molecules in the beam, which produces a strong ion signal in the central part of the image. To separate the signal from the relatively strong background, we alternate the relative timing of the photolysis and probe laser beams on an every other shot basis and accumulate each single image for 8−10 h. The real signal thus is the difference between one-laser signal where the probe laser leads the photolysis laser and two-laser signal in which the photolysis laser leads the probe laser. There are usually about 1500−2500 good ions left after the subtraction for each scan. Each DCS presented here is an average of approximately 5−10 scans done on different days.

III. THEORY

The quantum calculations of state-to-state DCSs were carried out using the time-dependent approach,[22] in which a quantum wave packet, containing a spread of collision energies, is propagated from the initial A + BC (H + D_2) to the final AC + B (HD + D) asymptotic arrangements of the reaction, employing the refined Boothroyd−Keogh−Martin−Peterson (BKMP2) potential energy surface,[1] although a more accurate potential is available.[23] The propagation of the wave packet was partitioned into three different stages, corresponding to the reactant, strong-interaction, and product regions of the reaction PES, which allows us to use a different basis set in each region; we used efficient basis sets constructed from grids based on H + D_2 Jacobi coordinates in the reactant region and HD + D Jacobi coordinates in the strong-interaction and product regions. Separate wave packet propagations were carried out for each value of the total angular momentum quantum number, J, for each initial rotational quantum number (j = 0, 1, 2) of the D_2 molecule, and for each value of its projection, Ω, onto the H + D_2 approach vector. Converged differential cross sections were obtained by including all partial waves in the range J = 0−55, with the maximum value of the projection of J on the approach velocity, Ω, set to 30. The parameters used in our calculations were sufficient to achieve convergence of the DCS over a continuous range of collision energies from 1.9 to 3.4 eV.

The experiment was carried out at a collision energy of 3.26 eV, which exceeds the energetic minimum of the conical

DOI: 10.1021/acs.jpca.5b04573
J. Phys. Chem. A 2015, 119, 12036−12042

intersection (CI) seam at 2.74 eV, but our calculations included neither the geometric phase (GP) nor the coupling to the first excited electronic state. The omission of these nonadiabatic effects is based on our previous findings[14] for the H + H_2 reaction, where substantial GP effects in the DCS start to appear only at total energies above 3.5 eV, indicating that only a very small portion of the dynamics passes over two transition states (which is necessary to produce encirclement of the CI and hence GP effects[14,19,24]). We expect similar behavior in the dynamics of the H + D_2 isotopologue considered here.

IV. RESULTS

A. Slow-Channel Correction. To compare the theoretically calculated DCSs with that of experimental measurements, we must blur the theoretical DCSs to account for the experimental conditions, i.e., (1) for the rotational energy spread of D_2 as it can be cooled only to $j \leq 2$ in the current experimental conditions and (2) the uncertainty in the collision energy (~0.05 eV) caused by imperfect translational cooling. In the present study these two conditions have been taken care of in the same way as in refs 7 and 10. The effect of the ionization recoil has been proven to be negligibly small.[7] In this section, we will mainly discuss how we corrected for the presence of the slow channel arising from slower H atoms in the photolysis of HBr that produces spin−orbit-excited Br atoms. Our procedure is different from the previous method that was presented in ref 7. When the fluorine excimer laser crosses with the molecular beam, it photodissociates HBr as shown below:

$$\mathrm{HBr} + h\nu_{157.64\mathrm{nm}} \rightarrow \mathrm{H} + \mathrm{Br} \quad \text{with } E_c = 3.26 \text{ eV}$$
$$\rightarrow \mathrm{H} + \mathrm{Br}^* \quad \text{with } E_c = 2.90 \text{ eV}$$

Here, E_c is the collision energy that is available for the H + D_2 → HD + D reaction and Br and Br* are the spin−orbit-ground and spin−orbit-excited levels of the bromine atom, respectively. We follow the usual practice of naming the dissociation channel that produces bromine atom in the ground state as the fast channel and the other as the slow channel.

Figure 1 shows the H atom speed distribution following the fluorine excimer laser photodissociation of HBr and [2 +1] REMPI detection of H atoms at 243.1 nm. The slow channel of HBr at 157.64 nm cannot be completely resolved from the fast channel, but appears as only a small bump at the foot of the large peak of the fast channel. The branching ratio qualitatively agrees with the theoretical calculation which predicts 84% in fast channel and 16% in slow channel, respectively.[25] The slow channel has a collision energy of 2.90 eV, which is still higher than all the previously investigated collision energies for this reaction, and has a reaction cross section comparable with that of the fast channel for the HD product states reported here. Therefore, it must be included when comparing the calculated DCSs with experimental ones. The difficulty here is that we do not have a way to produce relatively pure H atoms at E_c = 2.90 eV to be able to subtract its contribution from the E_c =3.26 eV DCS, a method we previously used for the slow-channel correction.[7]

Instead, we have decided to modify the theoretical data to simulate the experimental conditions. Consider the DCS of HD(v' = 3, j' = 8) as an example. In Figure 2a, the calculated absolute DCSs for the reaction H + D_2 → HD(v' = 3, j' = 8) + D at the collision energies of 3.26 eV (fast channel, red curve) and 2.90 eV (slow channel, blue curve) are shown, which have already been blurred according to the experimental conditions

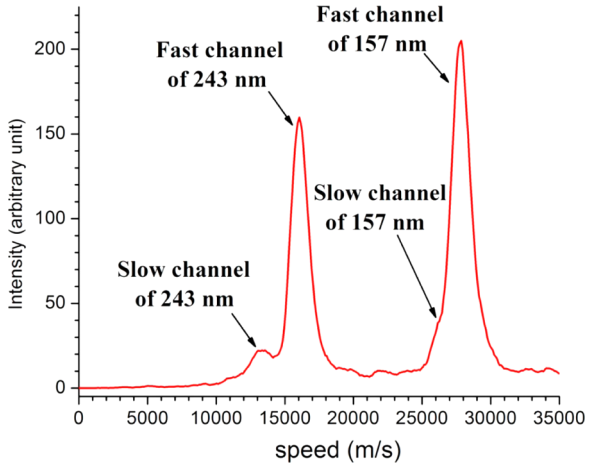

Figure 1. H atom speed distribution for the fluorine excimer photodissociation of HBr converted from the 3D ion image. The H atom is photoionized using [2 + 1] REMPI via the $2s(^2S_{1/2}) \leftarrow 1s(^2S_{1/2})$ transition at 243.1 nm. Powers of about 15 μJ/pulse and 300 μJ/pulse were used for the probe laser and fluorine excimer laser, respectively. The fast and slow channels corresponding to the probe laser and the fluorine excimer laser photodissociation of HBr are labeled by arrows.

mentioned above. As can been seen in Figure 2a, the slow channel has an absolute cross section that is higher than that of the fast channel; thus, we cannot ignore its contribution, even though it contributes only 16% to the total cross section. Experimentally we measured the lab-frame speed distribution of the HD products which are generated from both the fast and slow channels. Then we used the PHOTOLOC parameters (the center-of-mass speed and the speed of HD in the center-of-mass frame) of the fast channel to convert the speed distribution into the DCS. Therefore, it is not valid to add the two DCSs directly with weighting by the branching ratios of the fast and slow channels because the slow channel has PHOTOLOC parameters different than that of the fast channel. To simulate the experimental conditions, we first convert the two theoretical DCSs into speed distributions based on their corresponding cross sections and PHOTOLOC parameters, sum up the two speed distributions using branching ratios of the two channels [84(fast):16(slow)], and then convert the combined speed distribution into the DCS once again by using the PHOTOLOC parameters of the fast channel. In this way, we exactly simulated the experimental conditions, although at the expense of losing information on the absolute cross section. In Figure 2b, the modified DCS for HD(v' = 3, j' = 8) is presented. It has a dramatic change compared with the DCS (red curve in Figure 2a) without inclusion of the slow channel correction. In the following section, we will compare the experimental measurements with the theoretical DCSs that have been modified based on the method described above.

B. Experimental Data. The experimentally measured DCSs for the reaction H + D_2 → HD(v' = 3, j' = 4−10) + D are presented in Figure 3 by red dots. Owing to the strong noise generated by the fluorine excimer laser as described in the Experimental Section, for each single scan we must accumulate the image for 8−10 h, and each of the experimental DCSs showed in Figure 3 is an average of 5−10 different scans on different days depending on the signal level, with each scan having 1500−2500 good ions. To double-check if the

DOI: 10.1021/acs.jpca.5b04573
J. Phys. Chem. A 2015, 119, 12036−12042

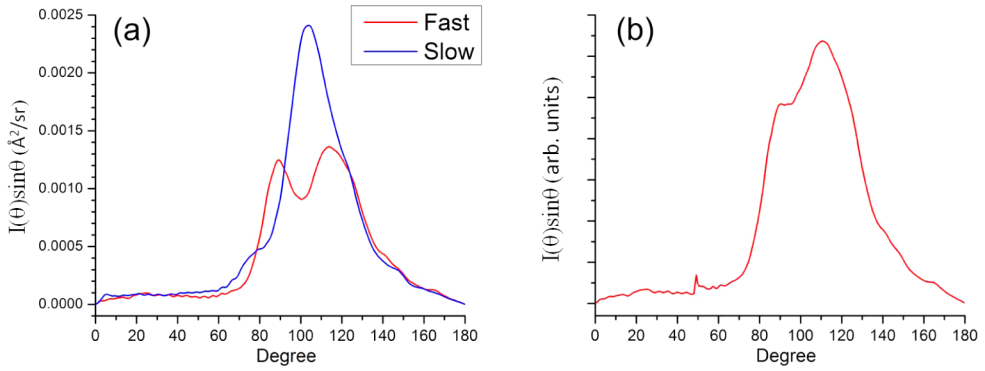

Figure 2. (a) Theoretical DCSs for the reaction of H + D_2 → HD(v' = 3, j' = 8) + D at the collision energies of 3.26 and 2.90 eV which corresponds to the fast (red curve) and slow channels (blue curve), respectively. The DCSs have already been blurred according to the fact that the D_2 molecules were populated by the j = 0, 1, and 2 rotational levels in the molecular beam and the collision energy has an uncertainty (~0.05 eV) originating from imperfect translational cooling. (b) DCS that includes the slow channel correction (see Experimental Section). The small step at ~50° is from the addition of the slow-channel reaction.

measurements are reproducible, several of the DCSs were repeated after several months, and the results were found to be similar to the previous measurements within the experimental errors. Here, all the experimental DCSs are separated into 40 angular bins, which has been shown to have enough angular resolution to resolve the fine structures in the DCSs while being small enough to reduce statistical uncertainties for each angular bin as well as being able to account for the photoionization recoil uncertainties of the product speed. The error bars in Figure 3 represent one standard deviation of the different independent scans. The theoretically calculated DCSs have been modified to simulate the experimental conditions as described above in Slow-Channel Correction (see Figure 2) and presented in Figure 3 using solid black lines. A least-squares fitting procedure[10,26] was performed to compare the theoretical calculations with experimental measurements. The fitting parameter R^2 value[26] is used to quantify the quality of the fitting process and to provide a measure of how well the theoretical DCSs agree with the experimental ones. A value of R^2 = 1 represents a perfect agreement. Table 1 lists the R^2 values for all the product states that are shown in Figure 3. All the R^2 values in Table 1 are greater than 0.91, indicating good overall agreement between theory and experiment.

V. DISCUSSION AND CONCLUSIONS

The good overall agreement between theory and experiment as presented in Figure 3 and Table 1 made us confident on both theoretical calculations and experimental measurements of the DCSs of the reaction H + D_2 → HD(v' = 3, j' = 4−10) + D at the collision energy of 3.26 eV. This study represents the first collaboration between theory and experiment on this benchmark system at a collision energy well above the conical intersection of the H_3 potential energy surface. The overall profiles of the DCSs shown in Figure 3 show several interesting trends. First, the HD product becomes more backward scattered as the product rotational excitation decreases. The DCS of HD(v' = 3, j' = 4) is centered at ~125°, while the DCS of HD(v' = 3, j' = 10) peaks at ~100°. This trend has been well-documented in most previous studies of this reaction at relatively low collision energies caused by the direct recoil mechanism.[7,8] Theoretical calculations, however, have shown that at high collision energies different collision mechanisms in addition to the direct recoil mechanism start to dominate the dynamics of this reaction,[27,28] and this experiment shows that the trend continues at collision energies well above the CI. Thus, the trend that product with higher rotational excitation is more sideways and forward scattered is not limited to the direct recoil mechanism but arises from the more general rule that products with more rotational excitation have relatively greater contribution from partial waves with large total angular momentum (large impact parameter) except at the limit of low product recoil energy.[29−31] As shown in our recent study,[28] partial waves with increasingly larger J (total angular momentum) start to contribute to the reaction through a T-shaped collision geometry, as shown in Figures 3 and 4 of ref 28, mechanism (1), a different reaction mechanism from the direct recoil mechanism.

Second, all the DCSs in the present study as shown in Figure 3 exhibit multimodal structures instead of a single peak as in most of the cases at low collision energy. For HD(v' = 3, j' = 4 and 5), there are three obvious peaks in the DCS. The peak in the most forward-scattered region reduces to a small bump on the left side of the main structure for HD(v' = 3, j' = 6) and almost disappears for higher j' states; as for HD(v' = 3, j' = 7−9), two peaks are seen, and for HD(v' = 3, j' = 10), there is only one dominant peak with the second peak reduced to a small bump in the forward-scattered region. This multimodal structure is predicted by theory and also very well reproduced by experimental measurements, as shown in Figure 3. However, this is not the first time we have seen this multimodal DCS for this reaction. We recently measured DCSs for HD(v' = 1, j' = 0−5) at 1.97 eV and found similar multimodal structures.[28] In 2008, Greaves et al.[27] reported the quasiclassical trajectory (QCT) calculations showing the presence of at least three new mechanisms in H + D_2 → HD(v' = 0, j' = 0) + D reaction at E_c = 1.85 eV. However, we found that the multimodal structures in the case of HD(v' = 1, j' = 0−5) at E_c = 1.97 eV result not just from different quasiclassical mechanisms identified in ref 27, but from a quantum interference between them, as was seen in only QM calculations, not in QCT calculations.[28] At the collision energy of 1.97 eV, the multimodal structure persists up to j' = 5 in the v' = 1 manifold, and is seen only for j' = 0, 1 for the v' = 3 manifold. In the v' = 1 manifold, as the product rotation or j' increases, some of the mechanisms are losing their specific identity and some of the interferences are progressively disappearing. As a result, the number of multimodal structures decreases gradually.[28] At the collision energy of 3.26 eV as studied in the present work, the multimodal structure happens

DOI: 10.1021/acs.jpca.5b04573
J. Phys. Chem. A 2015, 119, 12036−12042

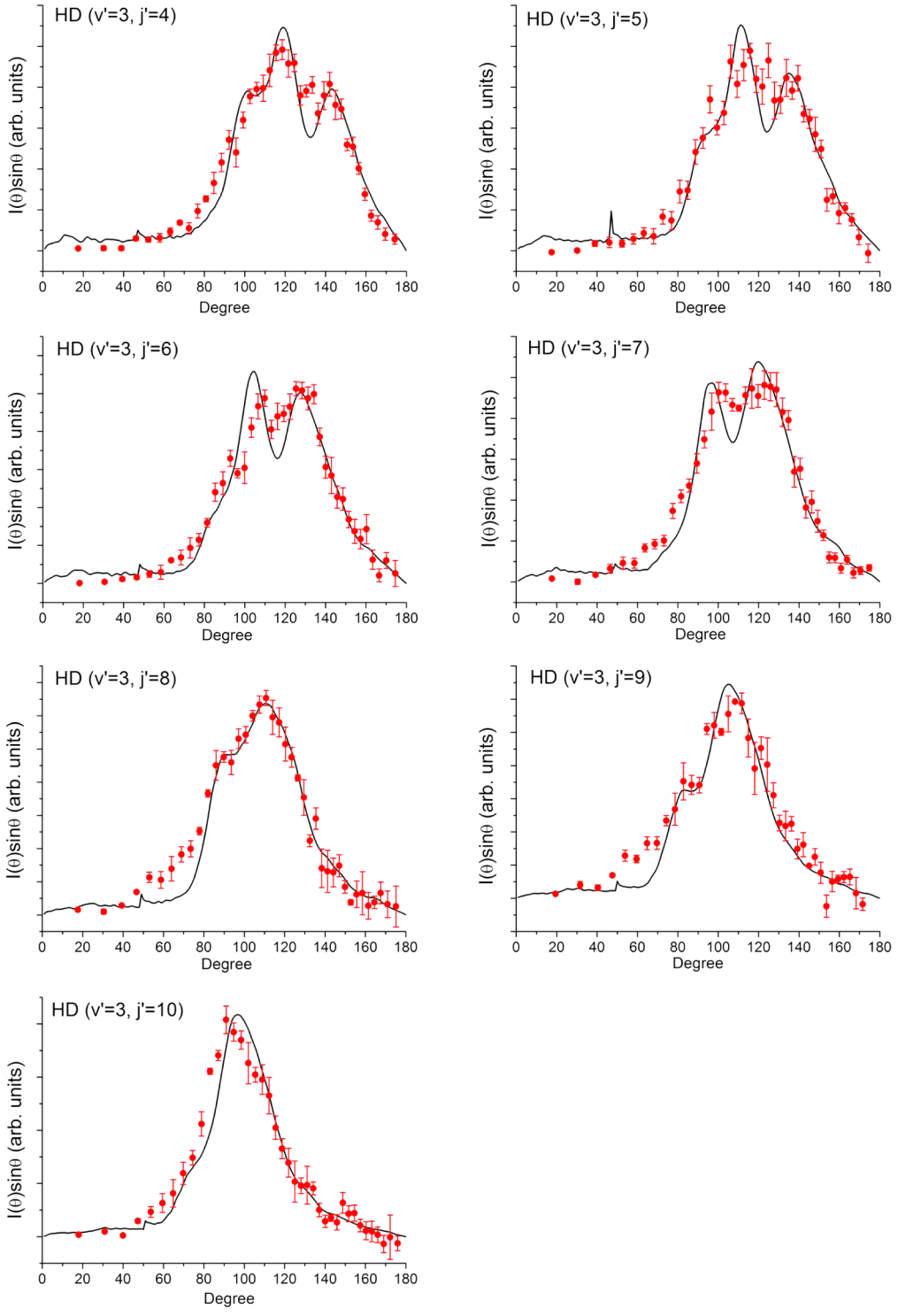

Figure 3. Experimental (red dots) and theoretical (solid black line) DCSs for the reaction H + D_2 → HD(v' = 3, j' = 4−10) + D at the collision energy of 3.26 eV. The theoretical DCSs have been modified to simulate the experimental conditions as described in the text. The error bars represent one standard deviation calculated from the statistical uncertainties in 5−10 different scans. The comparison is made by fitting the calculations with experiments through the least-squares fitting process.

Table 1. R^2 Values of the Least Squares Fitting Process between Theory and Experiment for H + D_2 → HD(v' = 3, j' = 4−10) + D DCSs at E_c = 3.26 eV, as Shown in Figure 3

HD(v' = 3, j')	j' = 4	j' = 5	j' = 6	j' = 7	j' = 8	j' = 9	j' = 10
R^2 value	0.9287	0.9179	0.9130	0.9365	0.9519	0.9109	0.9364

DOI: 10.1021/acs.jpca.5b04573
J. Phys. Chem. A 2015, 119, 12036−12042

in the $v' = 3$ manifold up to $j' = 10$, which is not seen at the collision energy of 1.97 eV in the same vibrational state. The trend that the number of fine peaks in the DCS decreases with increasing product rotational levels is consistent with that observed at low collision energies. Without the help of QCT calculations and partial wave analysis in QM calculations, it is hard to exactly identify what types of reaction mechanisms are present in this high-energy region and whether they quantum mechanically interfere with each other, but it is quite apparent that more than one mechanism is present in this case.

Lastly, we return to a consideration of the GP effect, which was one of the initial motivations for performing this experiment. We believe that the correct quantum treatment must include GP to make the wave function single-valued, but its inclusion causes a much more complicated theoretical treatment. In the current study, the theoretical calculations did not explicitly include the GP effect, but they nearly quantitatively agree with the experimental measurements, as can be seen from Figure 3 and Table 1. This implies that the GP effect is still not large enough at this collision energy to be identified experimentally. For the reaction H + H_2, which is an isotopic cousin of H + D_2, theoretical calculations with and without GP effect start to show prominent difference in the DCSs only at collision energies above 3.5 eV.[14] The present study proves that this behavior also applies to H + D_2. Thus, we need to go to even higher collision energies to be able to observe experimentally the GP effect. It also should be noted that the GP effect is not the only correction nor the most important one needed to account for nonadiabatic coupling effects.[32]

In summary, the present study has reported the first experimental measurements on the rovibrationally selected DCSs of the benchmark reaction system H + D_2 at the collision energy of 3.26 eV, which is well above the CI of H_3. The theoretical calculations without inclusion of the GP effect nearly quantitatively reproduce the experimental results, indicating that the GP effect does not play an important role in determining the form of the DCSs at this collision energy. Multimodal structures are observed up to $j' = 10$, but the number of fine peaks decreases with increasing product rotational excitation. Combined QM and QCT calculations are needed to understand the origins of those fine structures as observed in the DCSs in the present study.

AUTHOR INFORMATION

Corresponding Author

*E-mail: zare@stanford.edu.

Notes

The authors declare no competing financial interest.

ACKNOWLEDGMENTS

H.G., M.S., and R.N.Z. thank the U.S. National Science Foundation for support of this work (NSF CHE 1151428). S.C.A. acknowledges support from the U.K. Engineering and Physical Sciences Research Council. F.B. thanks the Max Born Institute in Berlin for financial support.

REFERENCES

(1) Boothroyd, A. I.; Keogh, W. J.; Martin, P. G.; Peterson, M. R. A Refined H_3 Potential Energy Surface. *J. Chem. Phys.* **1996**, *104*, 7139−7152.

(2) Schnieder, L.; Seekamp-Rahn, K.; Wrede, E.; Welge, K. H. Experimental Determination of Quantum State Resolved Differential Cross Sections for the Hydrogen Exchange Reaction H + D_2 → HD + D. *J. Chem. Phys.* **1997**, *107*, 6175−6195.

(3) Bañares, L.; Aoiz, F. J.; Herrero, V. J.; D'Mello, M. J.; Niederjohann, B.; Seekamp-Rahn, K.; Wrede, E.; Schnieder, L. Experimental and Quantum Mechanical Study of the H+D_2 Reaction Near 0.5 eV: The Assessment of the H_3 Potential Energy Surfaces. *J. Chem. Phys.* **1998**, *108*, 6160−6169.

(4) Wrede, E.; Schnieder, L.; Welge, K. H.; Aoiz, F. J.; Bañares, L.; Castillo, J. F.; Martínez-Haya, B.; Herrero, V. J. The Dynamics of the Hydrogen Exchange Reaction at 2.20 eV Collision Energy: Comparison of Experimental and Theoretical Differential Cross Sections. *J. Chem. Phys.* **1999**, *110*, 9971−9981.

(5) Harich, S. A.; Dai, D.; Wang, C. C.; Yang, X.; Chao, S. D.; Skodje, R. T. Forward Scattering Due to Slow-Down of the Intermediate in the H + HD → D + H_2 Reaction. *Nature* **2002**, *419*, 281−284.

(6) Althorpe, S. C.; Fernandez-Alonso, F.; Bean, B. D.; Ayers, J. D.; Pomerantz, A. E.; Zare, R. N.; Wrede, E. Observation and Interpretation of a Time-Delayed Mechanism in the Hydrogen Exchange Reaction. *Nature* **2002**, *416*, 67−70.

(7) Koszinowski, K.; Goldberg, N. T.; Zhang, J.; Zare, R. N.; Bouakline, F.; Althorpe, S. C. Differential Cross Section for the H + D_2 → HD(v'=1, j'=2,6,10) + D Reaction as a Function of Collision Energy. *J. Chem. Phys.* **2007**, *127*, 124315.

(8) Bartlett, N. C. M.; Jankunas, J.; Goswami, T.; Zare, R. N.; Bouakline, F.; Althorpe, S. C. Differential Cross Sections for H + D_2 → HD(v'=2, j'= 0,3,6,9) + D at Center-of-Mass Collision Energies of 1.25, 1.61, and 1.97 eV. *Phys. Chem. Chem. Phys.* **2011**, *13*, 8175−8179.

(9) Pomerantz, A. E.; Ausfelder, F.; Zare, R. N.; Althorpe, S. C.; Aoiz, F. J.; Bañares, L.; Castillo, J. F. Disagreement Between Theory and Experiment in the Simplest Chemical Reaction: Collision Energy Dependent Rotational Distributions for H + D_2 → HD(v'=3, j') + D. *J. Chem. Phys.* **2004**, *120*, 3244−3254.

(10) Jankunas, J.; Sneha, M.; Zare, R. N.; Bouakline, F.; Althorpe, S. C. Disagreement Between Theory and Experiment Grows with Increasing Rotational Excitation of HD(v', j') Product for the H + D_2 Reaction. *J. Chem. Phys.* **2013**, *138*, 094310.

(11) Mahapatra, S.; Köppel, H.; Cederbaum, L. S. Reactive Scattering Dynamics on Conically Intersecting Potential Energy Surfaces: The H + H_2 Exchange Reaction. *J. Phys. Chem. A* **2001**, *105*, 2321−2329.

(12) Ghosal, S.; Jayachander Rao, B.; Mahapatra, S. Reactive Chemical Dynamics Through Conical Intersections. *Proc. - Indian Acad. Sci., Chem. Sci.* **2007**, *119*, 401−407.

(13) Jayachander Rao, B.; Padmanaban, R.; Mahapatra, S. Non-adiabatic Quantum Wave Packet Dynamics of H+H_2 (HD) Reactions. *Chem. Phys.* **2007**, *333*, 135−147.

(14) Bouakline, F.; Althorpe, S. C.; Peláez Ruiz, D. Strong Geometric-Phase Effects in the Hydrogen-Exchange Reaction at High Collision Energies. *J. Chem. Phys.* **2008**, *128*, 124322.

(15) Herzberg, G.; Longuet-Higgins, H. C. Intersection of Potential Energy Surfaces in Polyatomic Molecules. *Discuss. Faraday Soc.* **1963**, *35*, 77−82.

(16) Mead, C. A.; Truhlar, D. G. On the Determination of Born-Oppenheimer Nuclear Motion Wave Functions Including Complications due to Conical Intersections and Identical Nuclei. *J. Chem. Phys.* **1979**, *70*, 2284−2296.

(17) Kendrick, B. K. Quantum Reactive Scattering Calculations for the D + H_2 → HD + H Reaction. *J. Chem. Phys.* **2003**, *118*, 10502−10522.

(18) Juanes-Marcos, J. C.; Althorpe, S. C. Geometric Phase Effects in the H + H_2 Reaction: Quantum Wave-Packet Calculations of Integral and Differential Cross Sections. *J. Chem. Phys.* **2005**, *122*, 204324.

(19) Juanes-Marcos, J. C.; Althorpe, S. C.; Wrede, E. Effect of the Geometric Phase on the Dynamics of the Hydrogen-Exchange Reaction. *J. Chem. Phys.* **2007**, *126*, 044317.

(20) Shafer, N. E.; Orr-Ewing, A. J.; Simpson, W. R.; Xu, H.; Zare, R. N. State-to-State Differential Cross Sections from Photoinitiated Bulb Reactions. *Chem. Phys. Lett.* **1993**, *212*, 155−162.

DOI: 10.1021/acs.jpca.5b04573
J. Phys. Chem. A 2015, 119, 12036−12042

(21) Koszinowski, K.; Goldberg, N. T.; Pomerantz, A. E.; Zare, R. N. Construction and Calibration of an Instrument for Three-Dimensional Ion Imaging. *J. Chem. Phys.* **2006**, *125*, 133503.
(22) Althorpe, S. C. Quantum Wavepacket Method for State-to-State Reactive Cross Sections. *J. Chem. Phys.* **2001**, *114*, 1601.
(23) Mielke, S. L.; Schwenke, D. W.; Schatz, G. C.; Garrett, B. C.; Peterson, K. A. Functional Representation for the Born-Oppenheimer Diagonal Correction and Born-Huang Adiabatic Potential Energy Surfaces for Isotopomers of H_3. *J. Phys. Chem. A* **2009**, *113*, 4479−4488.
(24) Bouakline, F.; Althorpe, S. C.; Larregaray, P.; Bonnet, L. Strong Geometric-Phase Effects in the Hydrogen-Exchange Reaction at High Collision Energies: II. Quasiclassical Trajectory Analysis. *Mol. Phys.* **2010**, *108*, 969−980.
(25) Smolin, A. G.; Vasyutinskii, O. S.; Balint-Kurti, G. G.; Brown, A. Photodissociation of HBr. 1. Electronic Structure, Photodissociation Dynamics, and Vector Correlation Coefficients. *J. Phys. Chem. A* **2006**, *110*, 5371−5378.
(26) Jankunas, J.; Sneha, M.; Zare, R. N.; Bouakline, F.; Althorpe, S. C. Simultaneous Measurement of Reactive and Inelastic Scattering: Differential Cross Section of the H + HD → HD(v', j') + H Reaction. *Z. Phys. Chem.* **2013**, *227*, 1281−1299.
(27) Greaves, S. J.; Murdock, D.; Wrede, E.; Althorpe, S. C. New, Unexpected, and Dominant Mechanisms in the Hydrogen Exchange Reaction. *J. Chem. Phys.* **2008**, *128*, 164306.
(28) Jambrina, P. G.; Herráez-Aguilar, D.; Aoiz, F. J.; Sneha, M.; Jankunas, J.; Zare, R. N. Quantum Interference between H + D_2 Quasiclassical Reaction Mechanisms. *Nat. Chem.* **2015**, DOI: 10.1038/nchem.2295.
(29) Jankunas, J.; Zare, R. N.; Bouakline, F.; Althorpe, S. C.; Herráez-Aguilar, D.; Aoiz, F. J. Seemingly Anomalous Angular Distributions in H + D_2 Reactive Scattering. *Science* **2012**, *336*, 1687−1690.
(30) Aldegunde, J.; Herráez-Aguilar, D.; Jambrina, P. G.; Aoiz, F. J.; Jankunas, J.; Zare, R. N. H + D_2 Reaction Dynamics in the Limit of Low Product Recoil Energy. *J. Phys. Chem. Lett.* **2012**, *3*, 2959−2963.
(31) Jankunas, J.; Sneha, M.; Zare, R. N.; Bouakline, F.; Althorpe, S. C.; Herráez-Aguilar, D.; Aoiz, F. J. Is the Simplest Chemical Reaction Really so Simple? *Proc. Natl. Acad. Sci. U. S. A.* **2014**, *111*, 15−2032.
(32) Rao, T. R.; Mahapatra, S. Nuclear Motion on the Orbitally Degenerate Electronic Ground State of Fully Deuterated Triatomic Hydrogen. *J. Chem. Phys.* **2011**, *134*, 204307.

DOI: 10.1021/acs.jpca.5b04573
J. Phys. Chem. A 2015, 119, 12036−12042